




Article

Photostimulation of Extravasation of Beta-Amyloid through the Model of Blood-Brain Barrier

Ekaterina Zinchenko ^{1,*}, Maria Klimova ¹, Aysel Mamedova ¹, Ilana Agranovich ¹, Inna Blokhina ¹, Tatiana Antonova ¹, Andrey Terskov ¹, Alexander Shirokov ^{1,2}, Nikita Navolokin ^{1,3}, Andrey Morgun ⁴, Elena Osipova ⁴, Elizaveta Boytsova ⁴, Tingting Yu ^{5,6}, Dan Zhu ^{5,6}, Juergen Kurths ^{1,7,8} and Oxana Semyachkina-Glushkovskaya ^{1,7,*}

¹ Department of Human and Animal Physiology, Saratov State University, Astrakhanskaya Str. 83, 410012 Saratov, Russia; mari-1997@mail.ru (M.K.); mamedovaysel95@gmail.com (A.M.); ilana.agranovich@yandex.ru (I.A.); inna-474@yandex.ru (I.B.); titatiana@gmail.com (T.A.); terskow.andrey@gmail.com (A.T.); shirokov_a@ibppm.ru (A.S.); nik-navolokin@yandex.ru (N.N.); juergen.kurths@pik-potsdam.de (J.K.)

² Institute of Biochemistry and Physiology of Plants and Microorganisms, Russian Academy of Sciences, Entusiastov Str. 13, 410049 Saratov, Russia

³ Department of Pathological Anatomy, Saratov State Medical University, 410010 Saratov, Russia

⁴ Research Institute of Molecular Medicine and Pathobiochemistry, Krasnoyarsk State Medical University named after Professor V. F. Voino-Yasenetsky, Partizana Zheleznyaka str., 1, 660022 Krasnoyarsk, Russia; 441682@mail.ru (A.M.); elena.hilazheva@mail.ru (E.O.); elizaveta.boicova@mail.ru (E.B.)

⁵ Britton Chance Center for Biomedical Photonics, Wuhan National Laboratory for Optoelectronics, Huazhong University of Science and Technology, Wuhan 430074, China; yutingting@hust.edu.cn (T.Y.); dawnzh@mail.hust.edu.cn (D.Z.)

⁶ MoE Key Laboratory for Biomedical Photonics, Collaborative Innovation Center for Biomedical Engineering, School of Engineering Sciences, Huazhong University of Science and Technology, Wuhan 430074, China

⁷ Physics Department, Humboldt University, Newtonstrasse 15, 12489 Berlin, Germany

⁸ Potsdam Institute for Climate Impact Research, Telegrafenberg A31, 14473 Potsdam, Germany

* Correspondence: Odonata1108@yandex.ru (E.Z.); glushkovskaya@mail.ru (O.S.-G.)

Received: 5 May 2020; Accepted: 22 June 2020; Published: 26 June 2020



Abstract: Alzheimer's disease (AD) is an incurable pathology associated with progressive decline in memory and cognition. Phototherapy might be a new promising and alternative strategy for the effective treatment of AD, and has been actively discussed over two decades. However, the mechanisms of therapeutic photostimulation (PS) effects on subjects with AD remain poorly understood. The goal of this study was to determine the mechanisms of therapeutic PS effects in beta-amyloid (A β)-injected mice. The neurological severity score and the new object recognition tests demonstrate that PS 9 J/cm² attenuates the memory and neurological deficit in mice with AD. The immunohistochemical assay revealed a decrease in the level of A β in the brain and an increase of A β in the deep cervical lymph nodes obtained from mice with AD after PS. Using the in vitro model of the blood-brain barrier (BBB), we show a PS-mediated decrease in transendothelial resistance and in the expression of tight junction proteins as well as an increase in the BBB permeability to A β . These findings suggest that a PS-mediated BBB opening and the activation of the lymphatic clearance of A β from the brain might be a crucial mechanism underlying therapeutic effects of PS in mice with AD. These pioneering data open new strategies in the development of non-pharmacological methods for therapy of AD and contribute to a better understanding of the PS effects on the central nervous system.

Keywords: Alzheimer's disease; transcranial photostimulation; lymphatic system; blood-brain barrier

1. Introduction

Alzheimer's disease (AD) is marked by a progressive decline in memory and cognition over decades. The beta amyloid ($A\beta$) hypothesis, which posits $A\beta$ deposition as a key initial step in the pathogenesis of AD, has been the dominant theory driving treatment development [1]. While the role of $A\beta$ in AD remains unclear, $A\beta$ plaque clearance has been a key target of numerous clinical trials. The one recent trial linked a significant reduction in $A\beta$ plaque to the stabilization of the cognitive decline after 1 year [2]. The blood–brain barrier (BBB) is a major obstacle for the effective delivery of therapeutic compounds for a treatment of AD. Therefore, the development of a non-pharmacological therapy of AD is actual problem. In our recent pilot study, we proposed transcranial photostimulation (PS) of clearance of $A\beta$ from the brain via a PS-mediated stimulation along the lymphatic pathway [3]. The PS known as low-level laser therapy is based on shining red lasers (600–700 nm) or near infrared light (760–1200 nm) onto the head via the intact scalp and the skull. The light penetrates into the brain where it is absorbed by specific chromophores that stimulates the generation of adenosine triphosphate and nitric oxide with an increase in energetic and metabolic capacities of the brain tissues [4]. We showed that the PS-stimulation of the reduction of $A\beta$ plaque in the brain induced an improvement of memory and neurocognitive deficit in mice with AD [3]. The PS-mediated improvement of memory and cognitive status in rodents with AD has been demonstrated in many other experimental investigations [5–8]. However, only a few studies have evaluated the mechanisms of therapeutic effects of PS in subjects with AD. In recent years, accumulating evidence has suggested that PS suppresses $A\beta$ -induced hippocampal neurodegeneration and long-term spatial and recognition memory impairments in rats that were injected bilaterally with $A\beta$ 1–42 to the hippocampus CA1 region [9]. Lu Y et al. revealed that $A\beta$ injection into the hippocampus led to mitochondrial abnormalities [6]. In contrast, PS is able to shift mitochondrial dynamics toward fusion by balancing the mitochondrial targeting fission proteins and fusion proteins [6]. Simultaneously, PS regulates the mitochondrial targeting ratio of active Bax/Bcl-2 and antioxidant level, intimating a vital role of PS in facilitating mitochondrial homeostasis and protection in hippocampal CA1 neurons [6]. The important restorative effects PS on the mitochondrial homeostasis as mechanisms of therapeutic effects of AD is discussed in other works [9,10].

In the last 5 years, the crucial role of the recently discovered meningeal lymphatic vessels (MLVs) in the development of AD and in the novel strategies of therapy of AD is debated in neuroscience [11]. Mesquita et al. demonstrate that augmentation of MLVs might be a promising therapeutic target for preventing or delaying age-associated neurological diseases [11]. In our recent studies we have shown that PS increases the permeability of the lymphatic endothelium and stimulates the lymphatic drainage function via a direct generation of singlet oxygen [12–14]. Based on these data, we hypothesize that PS can also affect the permeability of cerebral microvessels and the blood–brain barrier (BBB) that might be mechanism of a PS-mediated stimulation of lymphatic clearance of $A\beta$ from the brain. In our studies we clearly demonstrate that opening of BBB causes activation of drainage and clearing functions of MLVs [15–17], which is a pathway of $A\beta$ clearance [3,11]. It is interesting to note that the BBB disruption, even without pharmacological therapy, reduces $A\beta$ plaque in the mouse brain, triggers neuronal plasticity, and prevents spatial memory deficits [13–20]. Lipsman et al. reported intriguing data that suggest that MR-guided focused ultrasound opening of BBB is a promising novel method for therapy of patients with AD due to significantly reducing $A\beta$ plaque in the brain and improving the memory and neurocognitive status [21]. The above discussed facts give evidence to propose the involvement of BBB and MLVs in the therapeutic effects of PS in subjects with AD.

The aim of this article is to study the mechanisms of therapeutic PS effects in mice with AD with a focus on the investigation of PS-mediated influences on the BBB permeability for $A\beta$.

2. Materials and Methods

2.1. Subject

Experiments were performed in mongrel male mice (2 months old, weighing 20–25 g) in accordance with the Guide for the Care and Use of Laboratory Animals published by the US National Institutes of Health (NIH Publication No. 85–23, revised 1996). The mice were obtained from the vivarium of Saratov State University (Saratov, Russia) and housed in individually ventilated cages located in the specific pathogen free-grade facility. The protocols were approved by the Institutional Review Board of the Saratov State University (Protocol 7, 07.02.2017). The inclusion criteria were the normal behavior, neurocognitive and physiological status of mice, which were evaluated with a TSE Phenomster (TSE-System GmbH, Bad Homburg, Germany). The mice were housed at 25 ± 2 °C, 55% humidity, and 12:12 h light—dark cycle. Food and water were given ad libitum. After experiments, mice were killed using CO₂ easy box system for euthanasia (Rochaster Medical GmbH, Heitenried, Switzerland).

The study was conducted on 5 groups of animals: (1) group—the control (intact animals); (2) the sham group; (3) sham mice + PS; (4) mice with AD without PS; (5) mice with AD + PS, $n = 10$ –15 in each group in all sets of experiments.

2.2. The Injected Model of AD

The intrahippocampal injection of A β 1–42 (AS-6049101-0.1, A β -conjugated with cHiLyve™ TM Flour 488, Sigma-Aldrich, St. Louis, MO, USA) represents one of the most useful animal models of AD [22]. Since none of these available models fully represents the main pathological hallmarks of AD, injection of A β (1–42) into the hippocampus provides researchers with an in vivo alternative paradigm. The injected model of AD is the best-suited one for the studies of short-term effects of A β 1–42 on the brain functions and structures [22]. Here, we used the injected model of AD for the study of short-term effects of PS on the BBB integrity, the lymphatic clearance of A β (1–42) from the brain, and the memory and behavior status in mice. The modeling of AD was performed by intrahippocampal (the dentate gyrus field: ML \pm 1.3 mm, in AP—2.0 mm, DV—1.9 mm) injection of A β 1–42 (1 μ L). A β (1–42) was dissolved in phosphate saline buffer (PBS) to a final concentration of 50 μ M, followed by aggregation in a thermostat at 37 °C for 5–7 days. The sham group included mice with injection of physiological saline at a volume of 1 μ L into the hippocampus.

2.3. The Protocol of PS Course In Vivo and In Vitro Experiments

A fiber Bragg grating wavelength-locked high power static laser diode (LD-1267FBG-350, Innolume, Dortmund, Germany) emitting at 1267 nm (32 J/cm² on the skull and 9 J/cm² on the surface of the brain or for in vitro experiments) was described in our previous works [3,12,13]. The choice of the selected laser dose was determined by our recent data reporting the efficient PS dose for clearance of A β from the brain and for an increase in the lymphatic permeability [3,13]. The mice were recovered after the surgery procedure of injection of A β for 3 days. Afterward, mice were treated by PS for 9 days each second day under inhalation anesthesia (1% isoflurane at 1 L/min N₂O/O₂—70:30). The mice heads were shaved and fixed in a stereotaxic frame, and irradiated in the area of the sagittal and the triangle sinuses, where the rich network of the MLs are [23], using the sequence of: 17 min—irradiation, 5 min—pause for 61 min [3,12,13].

2.4. Memory and Neurological Tests

The behavioral tests were conducted from 3 days after the modeling of AD and for 9 days each second day. A detailed description of the behavior tests is presented in our previous publication [3]. Cages and equipment for these tests were cleaned between the tests to remove scents. The neurobehavioral status of mice was obtained by the neurological severity score (NSS). It consists of 9 individual parameters in points, including tasks on motor function, alertness and

physiological behavior. One point is assigned for failing the task, so a normal healthy animal should have 0 points for all points of the scale.

The new object recognition test was used for memory evaluation. This test is based on the desire of mice to explore a new object instead of a previously familiar one, which reflects the processes of study, recognition and memorization. The established protocol of novel object recognition test was described in Ref. [24]. On the first day, the mouse was placed in a cage ($47 \times 26 \times 20$ cm) and allowed to explore an open field for 5 min. On the second day, two identical novel objects (black cubes, $4 \times 4 \times 3$ cm) were placed in a cage and the mouse explored them for 10 min. After 1 h, one novel object (pink ball, 5 cm in diameter) and one familiar one (black cube) were presented to the mice and they were allowed to explore them for the next 5 min. The total time spent exploring the new and old objects was compared. Time for exploring an object (when the mouse's nose was directed at the object and less than approximately 2 cm from it) included time in direct contact and time within the object area. A discrimination index was calculated as the total time spent for exploring the new object divided by the total time devoted to exploration of all objects.

2.5. The BBB Model In Vitro

Cell culture models, based on immortalized brain endothelial cell lines, have been developed in order to facilitate in vitro studies of drug transport to the brain [25]. The best the BBB models in vitro which mimic the in vivo BBB integrity are characterized by high transendothelial electrical resistance (TEER regularity above $200 \text{ Ohm} \times \text{cm}^2$) and the expression of tight junction (TJ) proteins as critical factors of the BBB physiology and structure [26].

Brain microvessel endothelial cells (BMECs) were isolated from the brain of Wistar rats (postnatal day 10–14). Isolation and establishment of primary culture of BMECs were done according to the protocol of Liu et al. [27]. The BMECs obtained were phenotyped by the standard immunohistochemistry protocol using primary anti-ZO1 antibodies (Santa Cruz Biotechnology, Inc., Dallas, TX, USA, sc-8147) and secondary antibodies labeled with Alexa Fluor 488 (Abcam, Cambridge, UK, ab150117) followed by the detection with the fluorescent microscope. Astroglial and neuronal cells for the BBB model were obtained from embryonic rat neurospheres as described in [28]. The integrity of the in vitro BBB model containing BMECs monolayer grown on inserts, astrocytes and neurons grown in the well was confirmed with the TEER measurements.

2.6. Measurement of BBB Permeability

The TEER was measured using an EVOM2 volt-ohmmeter with the STX-2 chopstick electrodes (World Precision Instruments, Sarasota, FL, USA). Resistance values (Ωcm^2) were corrected by subtracting the resistance of an empty Transwell filter.

Primary antibodies to VE-Cadherin (Abcam, UK, ab205336); Claudin-5 (CLND, Abcam, UK, ab111336); zonula-1 (ZO-1, Abcam, UK, ab190085) were used for confocal analysis of expression of TJ proteins in the model of BBB. Primary antibodies were used in a working dilution of 1:300. The incubation time was 18 h at 4°C . Secondary antibodies were used in breeding 1:500 (donkey goat with Alexa 594 (Abcam, UK, ab150132); donkey rabbit with Alexa 488 (Abcam, UK, ab150073)—incubation time 2 h at a temperature of 37°C . The quantitative study of expression of the TJ proteins was carried out with the program ImageJ v1.43 using confocal photographic images (Leica TCS SP 5; Leica Microsystems Inc., Wetzlar, Germany).

2.7. Analysis of Level of $A\beta$ in the Tested Tissues

The deep cervical lymph nodes (dcLNs) are the first anatomical “station” for the cerebrospinal fluid outflow and clearance of macromolecules from the brain [3,12,13,16,29,30]. Here, we studied the clearance of $A\beta$ 1–42 from the brain in tested mice. The dcLNs were removed 9 days after intrahippocampal injection of $A\beta$ 1–42 (the AD group) or physiological saline (the sham group) as well as after the PS-course during 9 days (the AD + PS group) or immediately (the control group including

intact mice) and placed into 1% agarose for 1 day. The standard protocol of immunohistochemical (IHC) study was used with anti-A β antibody (1:500; Abcam, ab182136, Cambridge, UK). The samples were sectioned into 3 μ M to 5 μ M sections on a vibratome (Leica VT 1000S Microsystem) and were evaluated by light microscopy using a Mikrovizor μ Vizo-103 digital image medical analysis system (LOMO, Petrograd, Russia). Approximately 10 slices per animal were imaged. The quantitative analysis of the results of IHC staining on A β marker was carried out on a microscopic system with automatic analysis of the obtained photos of Ariol SL50 (Genetix, Newcastle on Tyne, UK). The total area of IHC was determined with the software module PathVysion (Music, Inc. Applied Imaging, Des Plaines, IL, USA).

A culture medium containing a fluorescently-labeled A β at a final concentration of 2 μ M was introduced into the culture insert with a monolayer of endotheliocytes (the model of BBB in vitro) (see Figure 1). After 1 h, 2 h, 4 h, 24 h, and 48 h, 100 μ L of medium was taken from the lower compartment of the well to determine the fluorescent amyloid passing through the endothelial monolayer. The A β concentration was determined using the program ImageJ v1.43 for confocal photographic images (Leica TCS SP 5; Leica Microsystems Inc., Weztlar, Germany).

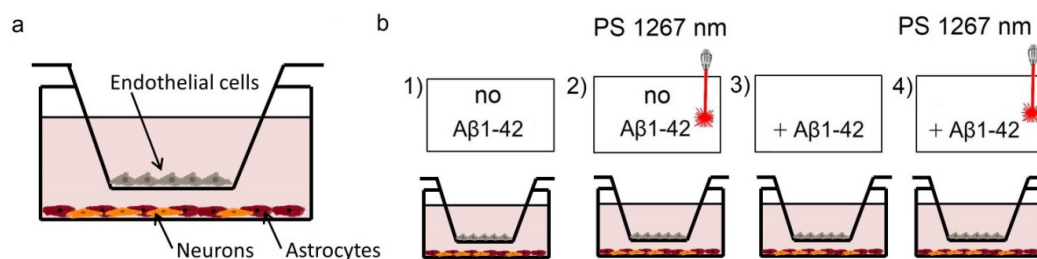


Figure 1. Schematic illustration of a three-cell model of a neurovascular unit (NVU) in vitro: (a) the cultivation and differentiation of cells of NVU: the formation of a monolayer of astrocytes occurs in 7–9 days; for neurons, in 10–14 days; and for endotheliocytes, in 7 days; (b) the experimental groups: (1) the control group, no A β 1–42 and PS; (2) photostimulation (PS) without application of A β 1–42; (3) application of A β 1–42 without PS; (4) A β 1–42 + PS.

2.8. Measure the Thermal Impact of PS

A type A-K3 thermocouple (Ellab, Hillerød, Denmark) was used to measure skull temperature. The thermocouple was placed subcutaneously on the bregma. A type A-K19 needle thermocouple (Ellab, Denmark) was used for the measuring of brain temperature. A burr hole was drilled under inhalation anesthesia (1% isoflurane at 1 L/min N₂O/O₂—70:30) with its center 2 mm lateral to the bregma and then thermocouple was inserted on the surface of the dura matter. The temperature in in vitro experiments was monitored under laser beam with TC-8 thermocouple Data Logger and PicoLog software (Pico Technology, Tyler, TX, USA).

2.9. Statistical Analysis

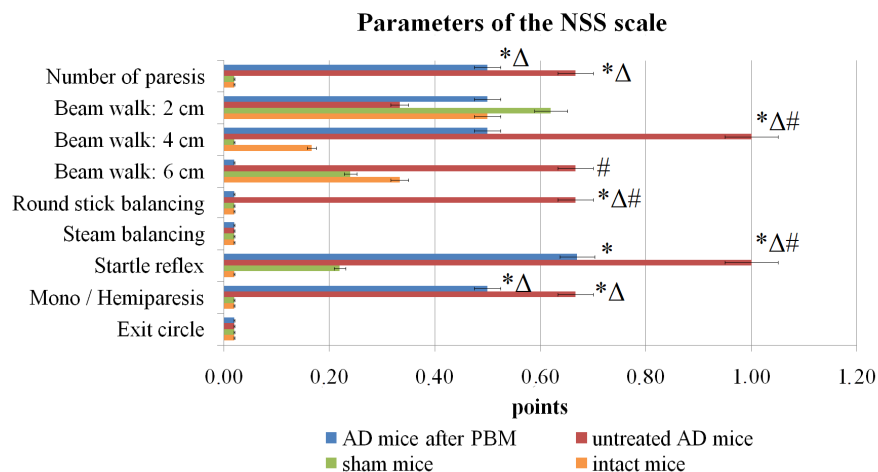
The results were reported as a mean value \pm standard error of the mean (SEM). Differences from the initial level in the same group were evaluated by the Wilcoxon test. Intergroup differences were evaluated using the Mann-Whitney test and the ANOVA-2 (post hoc analysis with the Duncan's rank test). The significance levels were set at $p < 0.05$ for all analyses.

3. Results

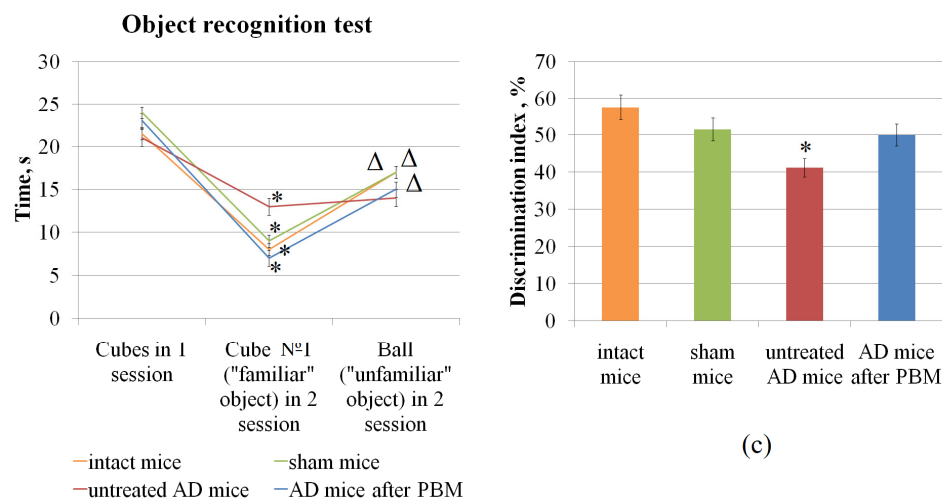
3.1. PS-Therapeutic Effects on the Memory and Neurological Deficit in Mice with AD

In the first step, we studied the memory and neurological impairment in mice with AD before and after PS. Figure 2a illustrates the NSS scale in the different groups (AD, AD + PS, and sham groups). Our results uncover a significant neurological deficit in mice with AD compared with sham

animals. Thus, mice with AD showed worse results than sham mice by the following indicators: mono/hemiparesis. Thus, A β injection has a significant pathogenic effect on the overall development of the sensory, motor, and coordinating sphere. The PS course improved the behavior status in mice with AD. Indeed, the performing tests for assessment of the neurological status (startle reflex, round stick balancing, beam walk (6; 4 cm)) was better in the AD + PS group vs. the AD group. Notice that the PS course did not influence the NSS scale in sham mice.



(a)



(b)

(c)

Figure 2. The PS effects on the memory and neurological status of mice with Alzheimer's disease (AD): (a) The assessment of the neurobehavioral status of mice on the NSS scale (*— $p < 0.05$ vs. intact mice; Δ — $p < 0.05$ vs. sham mice; #—between untreated AD mice and AD mice received PS); (b) The object recognition test, reflecting the processes of learning, recognition and memorization (*— $p < 0.05$ vs. cubes in 1 session; Δ — $p < 0.05$ vs. cube N°1 («familiar» object) in 2 session); (c) The discrimination index by the object recognition test (*— $p < 0.05$ vs. sham mice). $n = 10$ for each group.

In the novel object recognition test, sham mice spent more time exploring the novel subject than the familiar one that is typical sign of normal emotional response of mice to a new subject (Figure 2b). In the AD group, mice spend a similar amount of time exploring the new and the previous seen object, suggesting a memory deficit. However, in the AD + PS group the time of recognition of a new object was longer than in the AD group ($p < 0.01$, $n = 10$ in each group). The discrimination index (total time

for recognition of the new object/total time devoted to exploration of the new and familiar objects) was significantly smaller in the AD group compared with the sham group that was improved in the AD + PS group (Figure 2c).

3.2. PS-Course Causes Clearance of A β from the Brain in Mice with AD

In the second step, we analyzed the PS effects on clearance of A β from the brain using the intracranial hemorrhage (ICH) analysis of A β in the dcLNs. Figure 3a demonstrates that there are no A β plaques in the dcLNs in the sham groups. For A β , we found only a few plaques in the dcLNs in the AD group suggesting that AD is accompanied by a slow clearance of toxic protein from the brain that is consistent with the other results reporting the meningeal lymphatic pathway of A β clearance [11].

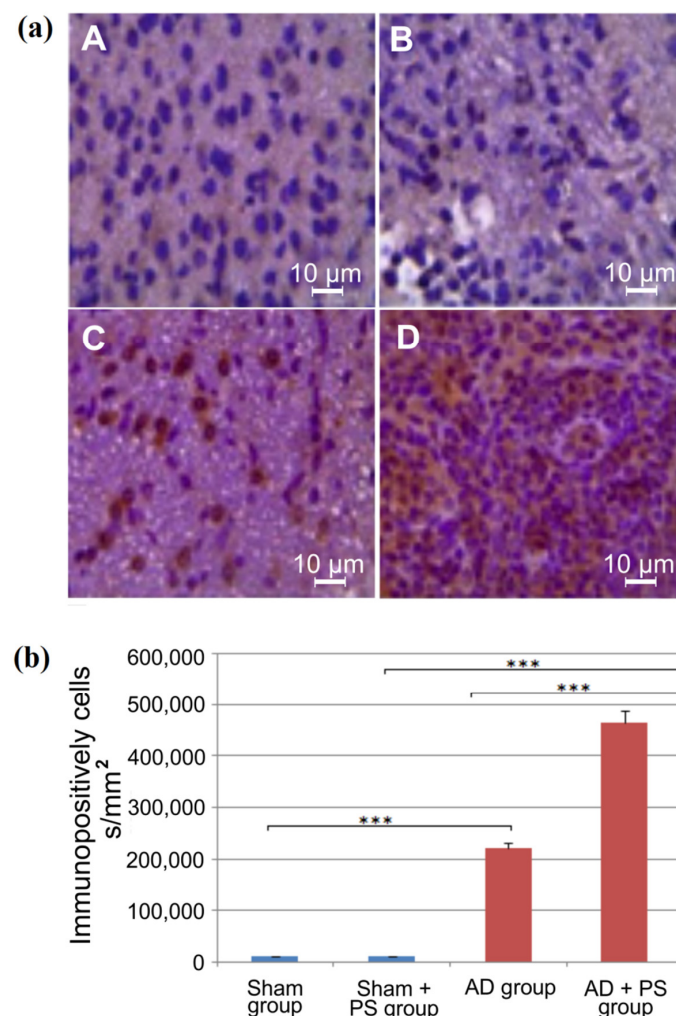


Figure 3. ICH analysis of A β plaques in the deep cervical lymph nodes (dcLNs) before and after PS: (a) A and B—ICH image does not show A β plaques in the dcLN in the sham groups; C and D—ICH image shows few A β plaques in the AD group and a significant A β level in the AD + PS group ($n = 10$ in each group); (b) The quantitative study of A β level in the dc LNs in the tested groups: ***— $p < 0.001$ vs. the sham groups, $n = 10$ in each group.

The AD + PS group demonstrated a pronounced A β level in the dcLNs compared with the AD group. This fact allowed us to conclude the effectiveness of the PS course for stimulation of clearance of A β from the brain in mice with AD. The quantitative analysis showed a higher signal intensity from immunopositive A β plaques in the dcLNs in the AD + PS group compared with the AD group and with sham mice (Figure 3b).

3.3. PS-Mediated Increase in the BBB Permeability

To better understand mechanisms of therapeutic PS effects in mice with AD, we examined the PS influences on the BBB permeability using the model of BBB. Lipsman et al. clearly showed that the BBB opening by focused ultrasound without any pharmacological interventions is associated with an improvement of the memory and the neurological status in patients with AD [21]. In our previous work we reported that the BBB opening causes activation of lymphatic clearance of the brain tissues from macromolecules crossed the BBB [17]. Based on these facts, we hypothesized that the PS-mediated opening of BBB might be one possible mechanism responsible for the activation of clearance of A β from the brain of mice with AD. To test this idea, we studied the PS effects on TEER and on the expression of an assembly of TJ proteins in normal mice as well as the PS effects on the A β leakage via the BBB in the sham and in the AD groups. Our results presented in Figure 4a show that PS induced an decrease in TEER. The expression of TJ proteins, such as CLND, VE-Cadherin and ZO-1, were significantly decreased after PS vs. the control group (Figure 4b). The reduced TEER and a decrease in the expression of TJ proteins indicate on the BBB opening [31,32] that suggests the PS-mediated increase in the BBB permeability. Figure 4c demonstrates that PS causes the BBB opening for fluorescent A β that was more pronounced in the AD + PS group compared with the sham group. There were no changes in the BBB permeability to A β in both the sham and AD groups. This finding indicates that A β itself does not affect the BBB integrity but the adding of A β in the endothelial cells decreases their resistance to PS-mediated influences on the BBB permeability that explains higher the BBB leakage to A β in the AD group vs. the sham group. The important role of the BBB in the development and progression of AD has also been shown by other researchers [33].

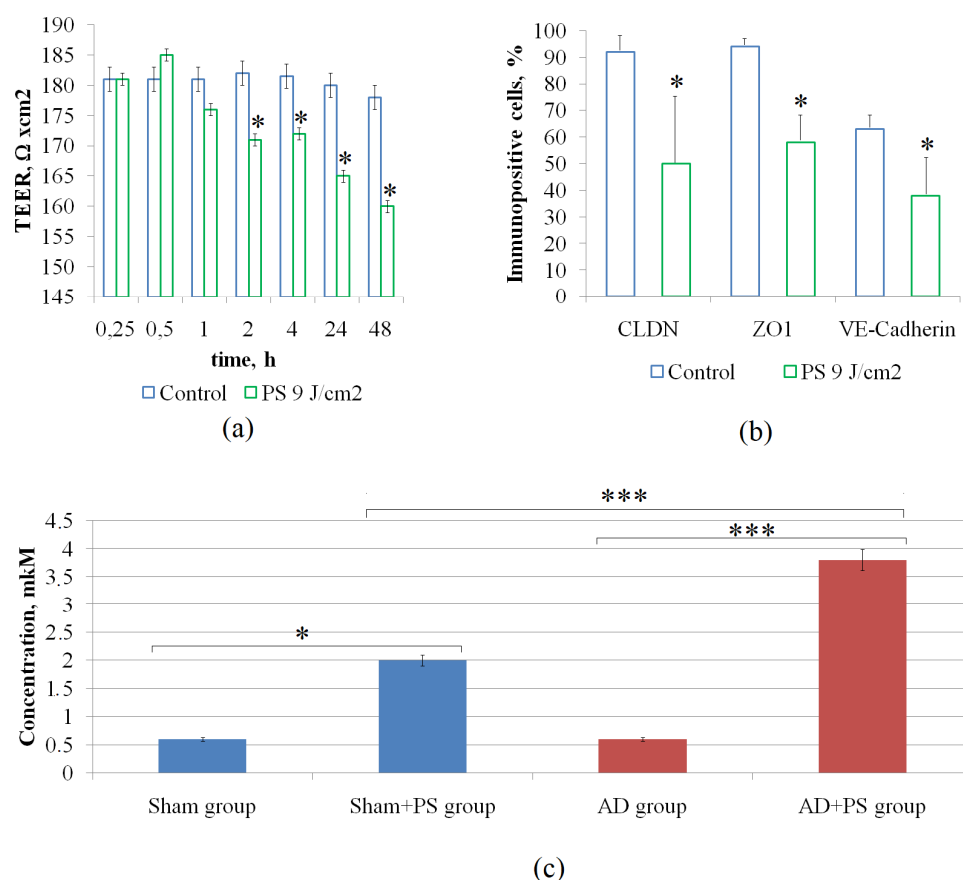


Figure 4. The PS-mediated effects on the blood-brain barrier (BBB) permeability: (a,b) The changes in transendothelial electrical resistance (TEER) and in the expression of tight junction (TJ) proteins before and after PS in normal mice, respectively; (c) The quantitative analysis of PS effects on the BBB permeability for fluorescent A β ; *— $p < 0.05$; ***— $p < 0.001$ vs. the sham groups, $n = 15$ for (a,b); $n = 10$ for (c).

3.4. The Thermal Impact of PS

The brain functions are very sensitive to the changes in the temperature. The increase of 0.5 °C causes the changes in the cellular level, and a 1 °C increase can have a profound effect on the neural network [34,35]. Therefore, we studied the effect of PS on the temperature on the skull and on the surface of the brain. Our results did not reveal any changes in the temperature on the skull's external surface (36.01 ± 0.11 vs. 36.11 ± 0.09 before and after PS, respectively) or on the cortical surface (37.12 ± 0.12 vs. 37.08 ± 0.10 before and after PS, respectively) after PS. In *in vitro* experiments the temperature in the BBB model did not change after PS (37.02 ± 0.04 and 37.05 ± 0.01 before and after PS, respectively).

4. Discussion

In this study, we analyzed the mechanisms responsible for the stimulatory PS effects on clearing A β from the brain associated with the improvement of memory and neurological deficit in mice with AD. The impact of direct infusion of A β into the hippocampus on the memory processes has been discussed in many studies [22,36]. However, in our experiments we revealed also the neurological deficit in the A β -injected mice. The results obtained from some patients with AD revealed that A β plaques do not necessarily precede the occurrence of cognitive declines [37,38]. Cognitively normal people can also have A β deposits in the brain [39,40]. These findings indicate that A β plaques may not always clinically correlate with AD. Thus, solute oligomeric species of A β 1–42, rather than A β plaques may be neurotoxic and responsible for synaptic and network dysfunctions [41–43]. Therefore, the intrahippocampal injection of solute A β might trigger multiple effects affecting diverse pathways leading gradually to the neurocognitive disorders, which depend on the site of injection and the nature of the peptide [44,45].

In our previous studies of the effects of different PS doses on the clearance of macromolecules from the brain such as dextran 70 kDa, A β and albumin complex of Evans Blue, we clearly show that the PS dose 9 J/cm² is most effective for the activation of lymphatic drainage and clearing functions [12,13]. We also found that the PS dose 9 J/cm² modulates the activity of factors responsible for the permeability of the lymphatic vessels [13]. Our pilot study demonstrates the effectiveness of the PS dose 9 J/cm² for a significant improvement of memory and neurological deficit in mice with AD [3]. These data are consistent with other results suggesting the therapeutic effects of PS on behavior status of mice and patients with AD [4–6]. However, the mechanisms underlying the PS therapy of AD remain poorly understood. This study is a continuation of a series of our experimental work, which is focused on the investigations of the mechanisms responsible for the PS-mediated improvement of symptoms of AD.

To confirm our previous data, here we demonstrate the effectiveness of PS 9 J/cm² in attenuation of the memory loss and neurocognitive deficit in mice with AD. Our ICH results uncover the lymphatic pathway of clearance of A β from the brain that is associated with the improvement of the behavior status of AD mice. The crucial role of the lymphatic system in the clearance of macromolecules and toxins from the brain has been shown in our previous [3,15–17] and other [11,29,30] experimental studies.

In our recent publications we also obtained that the PS dose 9 J/cm² increases the permeability of the lymphatic endothelium to macrophages via the changes of expression of TJ assembly and TEER [12,13]. Based on these data, we tested the hypothesis that PS can also affect the permeability of the cerebral blood vessels. Using the model of BBB in experiments *in vitro*, we found that PS 9 J/cm² decreases TEER and the expression of TJ proteins such as CLND, VE-Cadherin and ZO-1 suggesting the BBB opening [31,32]. Based on this fact, we analyzed the BBB permeability to fluorescent A β . Our confocal results demonstrate the leakage of A β through the BBB that was more pronounced in the group AD + PS compared with the sham + PS and the group AD. These results allow us to conclude that PS effectively increases the BBB permeability to A β . It is important to note that in our previous work we showed an urgent activation of the lymphatic clearance of macromolecules from the brain after the BBB opening by sound [17] or photodynamic effects [16]. We assume that the lymphatic system plays an important role in clearance of the brain tissues that has been shown also by others

reporting the involvement of the MLs in clearance of A β from the brain [11]. Thus, the PS-mediated BBB opening and associated with this activation of lymphatic clearance of A β from the brain might be a crucial mechanism explaining the PS-therapeutic effects on the memory and neurological deficit in mice with AD. Our conclusion also supports results reporting that the BBB disruption by focused ultrasound reduces A β plaque in the mouse brain, triggers neuronal plasticity, and prevents spatial memory deficits [18–20]. Lipsman et al. reported intriguing data that MR-guided focused ultrasound opening of BBB is a promising novel method for the therapy of patients with AD due to significantly reducing A β plaque in the brain and improving the memory and the neurocognitive status [21]. There is a limitation in our study. The PS effects on the memory and the neurological deficit as well as on the lymphatic clearance of A β from the brain was studied in mice with AD, while PS influences on the BBB permeability were evaluated using the BBB model cultured from rat endothelial cells. Murakami et al., using in situ brain perfusion technique, revealed that the drug permeation across the BBB is very similar in mice and rats despite the likely involvement of different transport mechanisms [46]. This fact allows us to compare the results obtained in our experiments in vivo and in vitro.

In summary, PS 9 J/cm² attenuates the memory and neurological deficit in mice with AD via activation of lymphatic clearance of A β from the brain into the dCLNs. The PS-mediated BBB opening via the PS-decrease TEER and the expression of TJ proteins might be a crucial mechanism underlying therapeutic effects of PS in mice with AD. These pioneering data open new strategies in the development of non-pharmacological methods for AD therapy and contribute to a better understanding of the PS effects on the central nervous system.

Author Contributions: Conceptualization, O.S.-G., D.Z., T.Y.; methodology, O.S.-G., E.Z.; validation, O.S.-G.; investigation, M.K., A.M. (Aysel Mamedova), I.A., I.B., T.A., A.T., A.S., N.N.; writing—original draft preparation, E.Z., M.K., A.S., N.N., A.M. (Andrey Morgun), E.O., E.B., T.Y.; writing—review and editing, O.S.-G., J.K.; visualization, E.Z.; supervision, O.S.-G., J.K.; project administration, D.Z., T.Y., O.S.-G. All authors have read and agreed to the published version of the manuscript.

Funding: This research was funded by grants from Russian Science Foundation (18-75-10033, 20-15-00090), Russian Foundation Fundamental Research (19-515-55016 China a) and RF Governmental Grant 075-15-2019-1885.

Conflicts of Interest: The authors declare no conflict of interest.

References

1. Karran, E.; De Strooper, B. The amyloid cascade hypothesis: Are we poised for success or failure? *J. Neurochem.* **2016**, *139*, 237–252. [[CrossRef](#)]
2. Sevigny, J.; Chiao, P.; Bussière, T.; Weinreb, P.; Williams, L.; Maier, M.; Dunstan, R.; Salloway, S.; Chen, T.; Ling, Y.; et al. The antibody aducanumab reduces A β plaques in Alzheimer's disease. *Nature* **2016**, *537*, 50–56. [[CrossRef](#)] [[PubMed](#)]
3. Zinchenko, E.M.; Navolokin, N.A.; Shirokov, A.A.; Khlebcev, B.N.; Dubrovsky, A.I.; Saranceva, E.I.; Abdurashitov, A.S.; Khorovodov, A.P.; Terskov, A.V.; Mamedova, A.T.; et al. Pilot study of transcranial photobiomodulation of lymphatic clearance of beta-amyloid from the mouse brain: Breakthrough strategies for nonpharmacologic therapy of Alzheimer's disease. *Biomed. Opt. Express* **2019**, *10*, 4003–4017. [[CrossRef](#)] [[PubMed](#)]
4. Lane, N. Cell biology: Power games. *Nature* **2006**, *443*, 901–903. [[CrossRef](#)] [[PubMed](#)]
5. Grillo, S.L.; Duggett, N.; Ennaceur, A.; Chazot, P. Non-invasive infra-red therapy (1072 nm) reduces β -amyloid protein levels in the brain of an Alzheimer's disease mouse model, TASTPM. *J. Photochem. Photobiol. B* **2013**, *123*, 13–22. [[CrossRef](#)] [[PubMed](#)]
6. Lu, Y.; Wang, R.; Dong, Y.; Tucker, D.; Zhao, N.; Ahmed, E.; Zhu, L.; Liu, T.C.-Y.; Cohen, R.M.; Zhang, Q. Low-level laser therapy for beta amyloid toxicity in rat hippocampus. *Neurobiol. Aging* **2017**, *49*, 165–182. [[CrossRef](#)] [[PubMed](#)]
7. De Taboada, L.; Yu, J.; El-Amouri, S.; Gattoni-Celli, S.; Richieri, S.; McCarthy, T.; Streeter, J.; Kindy, M. Transcranial laser therapy attenuates amyloid-beta peptide neuropathology in amyloid-beta protein precursor transgenic mice. *J. Alzheimer Dis.* **2011**, *23*, 521–535. [[CrossRef](#)] [[PubMed](#)]

8. Purushothuman, S.; Johstone, D.M.; Nandasena, C.; Van Eersel, J.; Ittner, L.M.; Stone, J. Near infrared light mitigates cerebellar pathology in transgenic mouse models of dementia. *Neurosci. Lett.* **2015**, *591*, 155–159. [[CrossRef](#)]
9. Gonzalez-Lima, F.; Barksdale, B.R.; Rojas, J.C. Mitochondrial respiration as a target for neuroprotection and cognitive enhancement. *Biochem. Pharmacol.* **2014**, *88*, 584–593. [[CrossRef](#)]
10. Grimm, A.; Friedland, K.; Eckert, A. Mitochondrial dysfunction: The missing link between aging and sporadic Alzheimer's disease. *Biogerontology* **2016**, *17*, 281–296. [[CrossRef](#)]
11. Da Mesquita, S.; Louveau, A.; Vaccari, A.; Smirnov, I.; Cornelison, R.C.; Kingsmore, K.M.; Contarino, C.; Onengut-Gumuscu, S.; Farber, E.; Raper, D.; et al. Functional aspects of meningeal lymphatics in ageing and Alzheimer's disease. *Nature* **2018**, *560*, 185–191. [[CrossRef](#)]
12. Semyachkina-Glushkovskaya, O.V.; Abdurashitov, A.S.; Dubrovsky, A.I.; Klimova, M.M.; Agranovich, I.M.; Terskov, A.V.; Shirokov, A.A.; Vinnik, V.V.; Kuznecova, A.S.; Lezhnev, N.D.; et al. Photobiomodulation of lymphatic drainage and clearance: Perspective strategy for augmentation of meningeal lymphatic functions. *Biomed. Opt. Express* **2020**, *11*, 725–734. [[CrossRef](#)] [[PubMed](#)]
13. Semyachkina-Glushkovskaya, O.V.; Abdurashitov, A.S.; Klimova, M.M.; Dubrovsky, A.I.; Shirokov, A.A.; Fomin, A.S.; Terskov, A.V.; Agranovich, I.M.; Mamedova, A.T.; Khorovodov, A.P.; et al. Photobiostimulation of cerebral and peripheral lymphatic functions. *Transl. Biophotonics* **2020**, *2*, e201900036. [[CrossRef](#)]
14. Sokolovski, S.G.; Zolotovskaya, S.A.; Goltsov, A.; Pourreynon, C.; South, A.P.; Rafailov, E.U. Infrared laser pulsetriggers increased singlet oxygen production in tumourcells. *Sci. Rep.* **2013**, *3*, 3484. [[CrossRef](#)] [[PubMed](#)]
15. Semyachkina-Glushkovskaya, O.V.; Chehonin, V.P.; Borisova, E.G.; Fedosov, I.V.; Namykin, A.A.; Abdurashitov, A.S.; Shirokov, A.A.; Khlebtsov, B.N.; Lyubun, E.V.; Navolokin, N.A.; et al. Photodynamic opening of the blood-brain barrier and pathways of brain clearing pathways. *J. Biophotonics* **2018**, *11*, e201700287. [[CrossRef](#)]
16. Semyachkina-Glushkovskaya, O.V.; Abdurashitov, A.S.; Dubrovsky, A.I.; Bragin, D.E.; Bragina, O.A.; Shushunova, N.A.; Maslyakova, G.N.; Navolokin, N.A.; Bucharskaya, A.B.; Tuchin, V.V.; et al. Application of optical coherent tomography for in vivo monitoring of the meningeal lymphatic vessels during opening of blood-brain barrier: Mechanisms of brain clearing. *J. Biomed. Opt.* **2017**, *22*, 121719. [[CrossRef](#)]
17. Semyachkina-Glushkovskaya, O.V.; Postnov, D.E.; Kurths, J. Blood–Brain Barrier, Lymphatic Clearance, and Recovery: Ariadne's Thread in Labyrinths of Hypotheses. *Int. J. Mol. Sci.* **2018**, *19*, 3818. [[CrossRef](#)]
18. Jordão, J.F.; Thévenot, E.; Markham-Coultes, K.; Scarcelli, T.; Weng, Y.-Q.; Xhima, K.; O'Reilly, M.; Huang, Y.; McLaurin, J.; Hynynen, K.; et al. Amyloid- β plaque reduction, endogenous antibody delivery and glial activation by brain-targeted, transcranial focused ultrasound. *Exp. Neurol.* **2013**, *248*, 16–29. [[CrossRef](#)]
19. Leinenga, G.; Götz, J. Scanning ultrasound removes amyloid- β and restores memory in an Alzheimer's disease mouse model. *Sci. Transl. Med.* **2015**, *7*, 278ra33. [[CrossRef](#)]
20. Burgess, A.; Dubey, S.; Yeung, S.; Hough, O.; Eterman, N.; Aubert, I.; Hynynen, K. Alzheimer disease in a mouse model: MR imaging-guided focused ultrasound targeted to the hippocampus opens the blood-brain barrier and improves pathologic abnormalities and behavior. *Radiology* **2014**, *273*, 736–745. [[CrossRef](#)]
21. Lipsman, N.; Meng, Y.; Bethune, A.J.; Huang, Y.; Lam, B.; Masellis, M.; Herrmann, N.; Heyn, C.; Aubert, I.; Boutet, A.; et al. Blood–brain barrier opening in Alzheimer's disease using MR-guided focused ultrasound. *Nat. Commun.* **2018**, *9*, 2336. [[CrossRef](#)] [[PubMed](#)]
22. Facchinetti, R.; Bronzuoli, M.R.; Scuderi, C. An Animal Model of Alzheimer Disease Based on the Intrahippocampal Injection of Amyloid β -Peptide (1–42). *Methods Mol. Biol.* **2018**, *1727*, 343–352. [[CrossRef](#)]
23. Ahn, J.H.; Cho, H.; Kim, J.H.; Kim, S.H.; Ham, J.S.; Park, I.; Suh, S.H.; Hong, S.P.; Song, J.H.; Hong, Y.K.; et al. Meningeal lymphatic vessels at the skull base drain cerebrospinal fluid. *Nature* **2019**, *572*, 62–66. [[CrossRef](#)] [[PubMed](#)]
24. Bevins, R.A.; Besheer, J. Object recognition in rats and mice: A one-trial nonmatching-to-sample learning task to study 'recognition memory'. *Nat. Protoc.* **2006**, *1*, 1306–1311. [[CrossRef](#)] [[PubMed](#)]
25. Garberg, P.; Ball, M.; Borg, N.; Cecchelli, R.; Fenart, L.; Hurst, R.D.; Lindmark, T.; Mabondzo, A.; Nilsson, J.E.; Raub, T.J.; et al. In Vitro Models for the Blood-Brain Barrier. *Toxicol. Vitro* **2005**, *19*, 299–334. [[CrossRef](#)] [[PubMed](#)]
26. Wilhelm, I.; Fazakas, C.; Krizbai, I.A. In Vitro Models of the Blood-Brain Barrier. *Acta Neurobiol. Exp. Wars* **2011**, *71*, 113–128.

27. Liu, Y.; Xue, Q.; Tang, Q.; Hou, M.; Qi, H.; Chen, G.; Chen, W.; Zhang, J.; Chen, Y.; Xu, X.-Y. A simple method for isolating and culturing the rat brain microvascular endothelial cells. *Microvasc. Res.* **2013**, *90*, 199–205. [\[CrossRef\]](#)
28. Khilazheva, E.D.; Boytsova, E.B.; Pozhilenkova, E.A.; Solonchuk, Y.R.; Salmina, A.B. Obtaining a three-cell model of a neurovascular unit in vitro. *Cell Tissue Biol.* **2015**, *9*, 447–451. [\[CrossRef\]](#)
29. Louveau, A.; Smirnov, I.; Keyes, T.J.; Eccles, J.D.; Rouhani, S.J.; Peske, J.D.; Derecki, N.C.; Castle, D.; Mandell, J.W.; Lee, K.S.; et al. Structural and functional features of central nervous system lymphatic vessels. *Nature* **2015**, *523*, 337–341. [\[CrossRef\]](#)
30. Aspelund, A.; Antila, S.; Proulx, S.T.; Karlsen, T.V.; Karaman, S.; Detmar, M.; Wiig, H.; Alitalo, K. A dural lymphatic vascular system that drains brain interstitial fluid and macromolecules. *J. Exp. Med.* **2015**, *212*, 991–999. [\[CrossRef\]](#)
31. De Boer, A.G.; Gaillard, P. The blood-brain barrier and drug transport to the brain. *STP Pharma Sci.* **2002**, *12*, 229–234.
32. Greene, C.; Campbell, M. Tight junction modulation of the blood brain barrier: CNS delivery of small molecules. *Tissue Barriers* **2016**, *4*, e1138017. [\[CrossRef\]](#) [\[PubMed\]](#)
33. Cai, Z.; Qiao, P.-F.; Wan, C.-Q.; Cai, M.; Zhou, N.-K.; Li, Q. Role of Blood-Brain Barrier in Alzheimer's Disease. *J. Alzheimer Dis.* **2018**, *63*, 1223–1234. [\[CrossRef\]](#) [\[PubMed\]](#)
34. Hoffmann, H.M.; Dionne, V.E. Temperature dependence of ion permeation at the endplate channel. *J. Gen. Physiol.* **1983**, *81*, 687–703. [\[CrossRef\]](#)
35. Moser, E.; Mathiesen, I.; Andersen, P. Association between brain temperature and dentate field potentials in exploring and swimming rats. *Science* **1993**, *259*, 1324–1326. [\[CrossRef\]](#)
36. Faucher, P.; Mons, N.; Micheau, J.; Louis, C.; Beracochea, D.J. Hippocampal Injections of Oligomeric Amyloid β -peptide (1–42) Induce Selective Working Memory Deficits and Long-lasting Alterations of ERK Signaling Pathway. *Front. Aging Neurosci.* **2016**, *7*, 245. [\[CrossRef\]](#)
37. Terry, R.D.; Masliah, E.; Salmon, D.P.; Butters, N.; DeTeresa, R.; Hill, R.; Hansen, L.A.; Katzman, R. Physical basis of cognitive alterations in Alzheimer's disease: Synapse loss is the major correlate of cognitive impairment. *Ann. Neurol.* **1991**, *30*, 572–580. [\[CrossRef\]](#)
38. Andreasen, N.; Blennow, K. CSF biomarkers for mild cognitive impairment and early Alzheimer's disease. *Clin. Neurol. Neurosurg.* **2005**, *107*, 165–173. [\[CrossRef\]](#)
39. Nordberg, A. Amyloid imaging in Alzheimer's disease. *Neuropsychologia* **2008**, *46*, 1636–1641. [\[CrossRef\]](#)
40. Villemagne, V.L.; Pike, K.E.; Darby, D.; Maruff, P.; Savage, G.; Ng, S.; Ackermann, U.; Cowie, T.F.; Currie, J.; Chan, S.G.; et al. Abeta deposits in older non-demented individuals with cognitive decline are indicative of preclinical Alzheimer's disease. *Neuropsychologia* **2008**, *46*, 1688–1697. [\[CrossRef\]](#)
41. Cleary, J.P.; Walsh, D.M.; Hofmeister, J.J.; Shankar, G.M.; Kuskowski, M.A.; Selkoe, D.J.; Ashe, K.H. Natural oligomers of the amyloid-beta protein specifically disrupt cognitive function. *Nat. Neurosci.* **2005**, *8*, 79–84. [\[CrossRef\]](#)
42. Haass, C.; Selkoe, D. Soluble protein oligomers in neurodegeneration: Lessons from the Alzheimer's amyloid beta-peptide. *Nat. Rev. Mol. Cell Biol.* **2007**, *8*, 101–112. [\[CrossRef\]](#)
43. Benilova, I.; Karran, E.; De Strooper, B. The toxic Abeta oligomer and Alzheimer's disease: An emperor in need of clothes. *Nat. Neurosci.* **2012**, *15*, 349–357. [\[CrossRef\]](#) [\[PubMed\]](#)
44. Mucke, L.; Selkoe, D. Neurotoxicity of amyloid beta-protein: Synaptic and network dysfunction. *Cold Spring Harb. Perspect. Med.* **2012**, *27*, a006338. [\[CrossRef\]](#)
45. Chambon, C.; Wegener, N.; Gravius, A.; Danyasz, W. Behavioural and cellular effects of exogenous amyloid-beta peptides in rodents. *Behav. Brain Res.* **2011**, *225*, 623–641. [\[CrossRef\]](#) [\[PubMed\]](#)
46. Murakami, H.; Takanaga, H.; Matsuo, H.; Ohtani, H.; Sawada, Y. Comparison of Blood-Brain Barrier Permeability in Mice and Rats Using in Situ Brain Perfusion Technique. *Am. J. Physiol. Heart Circ. Physiol.* **2000**, *279*, H1022–H1028. [\[CrossRef\]](#)

